Nigerian Journal of Technology (NIJOTECH)
Vol. 41, No. 3, May, 2022, pp.429-437
www.nijotech.com

Print ISSN: 0331-8443
Electronic ISSN: 2467-8821
http://dx.doi.org/10.4314/njt.v41i3.2

Modelling of the Temperature Profile of Heat Sinks for a Thermoelectric Cooler Module

F. Onoroh[1*], M. Ogbonnaya[2], L. O. Agberegha[3]

[1,2] *Department of Mechanical Engineering, University of Lagos, Akoka, Yaba, Lagos State, NIGERIA*
[3]*Department of Mechanical Engineering, Federal University of Petroleum Resources Effurun, Delta state, NIGERIA*

Abstract
Thermoelectric refrigeration achieves cooling through Peltier and Seebeck effect. Heat sinks attached to the hot and cold sides of the thermoelectric module help to efficiently dissipates and absorb heat. This research modelled the temperature profile across a heat sink and its optimization for a thermoelectric refrigeration application. Simulation was carried out using MATLAB to visualize the performance of the heat sink. The optimization was done using FMINCON in MATLAB by setting upper and lower bounds to satisfy space and volume requirement. The optimum values for the hot and cold heat sink geometry obtained using FMINCON tool in OPTIMTOOL box in MATLAB, yields number of fins as 10, fin spacing as 0.003m, the fin thickness as 0.002m and fin length as 0.015m with an optimum temperature of -0.8639.

Keywords: Heat sink; Peltier effect; Seebeck effect; Temperature profile; Fin spacing; Fin thickness; Fin length.

1.0 INTRODUCTION

Thermoelectric effect was first discovered by a French physicist, Jean Charles Athanase Peltier in 1834 [1]. He discovered that when a current is made to flow through a junction between two conductors of different materials p and n, that there is an increase in temperature at one end of the junction and a decrease in temperature at the other end of the junction depending on the direction of flow of current [2-3]. Modern thermoelectric cooler uses thermoelectric cooler modules which are made of semiconductor materials. The modules are sandwiched between heat sinks to enhance thermal dissipation and absorption from the modules [4]. Fourier's law of heat transfer reduced to Laplace equation shows that temperature differential in a heat sink causes heat to be transferred from a high to a low temperature region [5]. The heat transfer rate is directly proportional to the temperature gradient and cross sectional area through which heat is transferred.

A number of studies exist in the literature of heat sinks and thermoelectric refrigeration. Karathanassis et al [6] studied an optimization methodology for a micro channel plate-fin heat sink suitable for cooling of a linear parabolic trough concentrating photovoltaic/thermal system. Their analysis demonstrates that micro heat sinks achieve very low values of thermal resistance and that the use of variable-width channels significantly reduce the pressure drop of the coolant. Badgujar et al [5] studied the application of heat sink in thermoelectric cooler to dissipate 35 W of energy to obtain a desired refrigeration effect. Their finding showed that pressure drop is an important parameter governing the performance of the heat sink in forced convection.

Raju etal [7] designed and developed a solar thermoelectric refrigerator to produce refrigerating effect using solar energy. Experimental testing indicates a temperature reduction of 15oC from a ambient condition of 25oC using 500 ml of water. Lee et al [8] proposed a correlation for determining Nusselt number using experimental data for vertical cylinders with triangular fins applicable to natural convection. The contour map obtained shows the existence of fin number and fin thickness for minimal thermal resistance. They observed that the actual convection flow velocity through fins is usually unknown and is one of the parameters that affect thermal performance of the heat sink.

Micheli et al [9] worked on the thermal performance of plate and pin micro fin arrays in free convection. They showed that the efficiency of pin micro fins is greater than that of plate fin and that pin micro fins require less material for its manufacture. Yu et al [10] numerically and experimentally worked on a modern design

*Corresponding author **(Tel:** +234 (0) 8074648666**)**

Email addresses: fonoroh@unilag.edu.ng (F. Onoroh); mogbonnaya@unilag.edu.ng (M. Ogbonnaya); and agberegha.larry@fupre.edu.ng (L. O. Agberegha)

of plate pin heat sink, based on addition of column shaped pins staggered between plate fins to a simple plate fin heat sink. On comparing the thermal resistance between the plate pin fins and plate fins, they found that plate pins thermal resistance is lower by 30%. The performance of a thermoelectric generator (TEG) in combination with air cooler using two stage optimization was investigated by Wang et al [11]. Analytical method was used to model the heat transfer of the heat sink and a finite element scheme is employed for the performance of the TEG, with the TEG output increasing by 88.7%.

Szodrai [12] examined geometrics of heat sinks varying the temperature, relative humidity and flow rates with Ansys Fluent. The favourable geometry was chosen by Pareto-vector length optimization with 108 cases on 40 finned heat sinks with differing fin width. He employed TEC1-12706 thermoelectric cooling modules on a prototype and found out that the differential between simulated cool air and measured temperatures is 3%. Lin and Kiflemariam [13] developed a general numerical methodology and validation for the simulation of steady as well as transient thermal and electrical behaviours of thermoelectric generator based air flow self-cooling systems. A parametric study to determine the effect of heat sink geometry and thermoelectric generator arrangements on device temperature and power produced by the device showed that an increase in fin density results in a rise in fan power consumption, increase in net power and decrease in thermal resistance.

From the above, it is clear that various work has been done on different aspect of heat sink geometries and thermoelectric refrigeration, however exact analytical method of heat sinks coupled to a thermoelectric cooler module has not been widely documented. This present study developed a mathematical model of a heat sink directly coupled to a thermoelectric cooler module used to predict the temperature profile of hot and cold side of the modules using exact solutions. A rectangular plate heat sink of length 200mm and width 80mm, that encloses ten 40mm x 40mm thermoelectric module was studied. The results of the investigation can be practically used in cooling system applications in micro electro mechanical systems (MEMS).

2.0 DERIVATION OF HEAT TEMPERATURE PROFILE OF HEAT SINK

Figure 1 illustrates the principle of the Peltier effect. The heat absorbed or dissipated increases as the current supplied increases. Its figure of merit is expressed mathematically as [14]:

$$Z = \frac{\alpha^2}{\rho k} \tag{1}$$

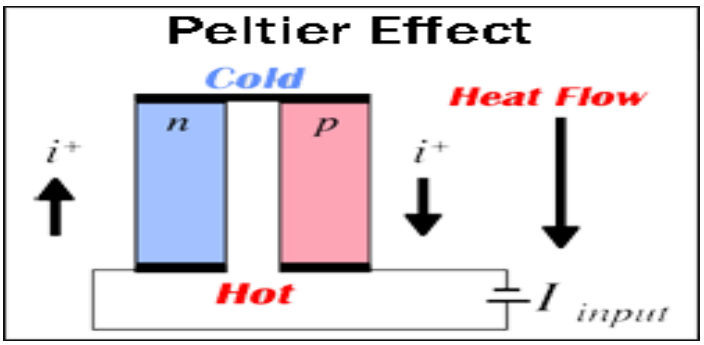

***Figure 1**: Peltier Effect [3]*

where α: Seebeck coefficient, V/K, ρ: electrical resistivity, Ωm, k: thermal conductivity, W/mK. It can also be obtained from the relation [15]:

$$Z = \frac{\alpha^2 \sigma}{k} \tag{2}$$

where σ: the electrical conductivity, S/m. The dimensionless figure of merit is defined as

$$ZT = \frac{\alpha^2 \sigma T}{k} \tag{3}$$

where T: absolute temperature, K. For improve performance of the thermoelectric modules, the Seebeck coefficient and the electrical conductivity should have high value and the thermal conductivity should have a low value [16-18]. Figure 2 depicts a rectangular fin heat sink in an environment whose atmospheric temperature is at T∞.

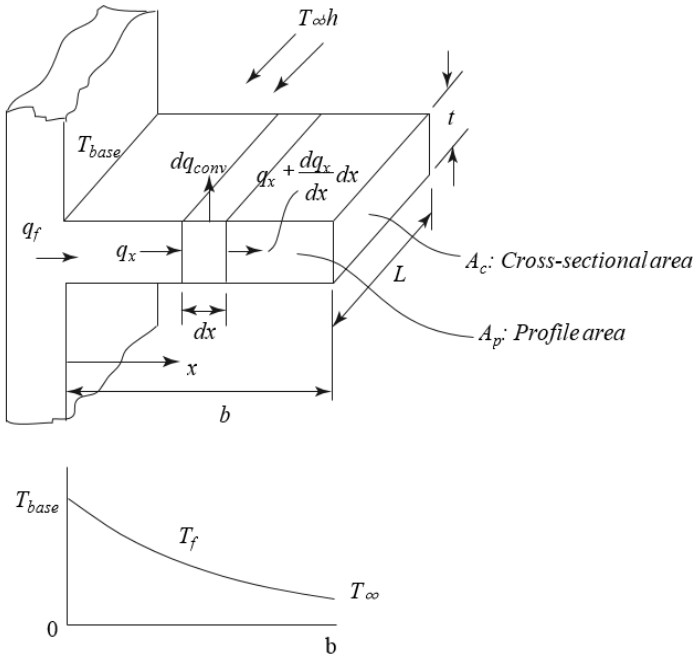

***Figure 2:** Plate Fin Temperature Distribution [19]*

Rate of heat conduction into the element at x, can be expressed as [20-21]:

$$Q_{cond\,x} = Q_{cond\,x+\Delta x} + Q_{conv} \quad (4)$$

Where $Q_{cond\,x+\Delta x}$ is rate of heat conduction from element at (x+Δx) ,W, Q_{conv} is rate of heat convection from the element ,W. Expanding $Q_{cond\,x+\Delta x}$ using Taylor series, the convective heat transfer can be obtained as:

$$Q_{conv} = Q_{cond\,x} + \frac{dQ_{cond\,x}}{dx}dx - Q_{cond\,x} \quad (5)$$

Therefore,

$$Q_{conv} = \frac{dQ_{cond\,x}}{dx}dx \quad (6)$$

Application of Fourier's law of conduction and Newton's law of cooling to equation (6) gives;

$$hPdx(T - T_\infty) - \frac{d}{dx}\left(kA_c\frac{dT}{dx}\right)dx = 0 \quad (7)$$

Which can be expressed as:

$$kA_c\frac{d^2T}{dx^2} - hP(T - T_\infty) = 0 \quad (8)$$

where P: perimeter of the fin, m. Equation (8) can be re-arranged as:

$$\frac{d^2T}{dx^2} - \frac{hP(T - T_\infty)}{kA_c} = 0 \quad (9)$$

Introducing the non-dimensional temperature, θ, defined as;

$$\theta = \frac{T - T_\infty}{T_b - T_\infty} \quad (10)$$

Upon rearrangement gives;

$$T = T_\infty + (T_b - T_\infty)\theta \quad (11)$$

Introducing the non-dimensional length, X, defined as;

$$X = \frac{x}{L} \quad (12)$$

Where L is the length of fin, m. In the light of equation (11) and equation (12), equation (9) can readily be expressed as:

$$\frac{d^2}{d(XL)^2}(T_\infty + (T_b - T_\infty)\theta) - \frac{hP}{kA_c}((T_\infty + (T_b - T_\infty)\theta) - T_\infty) = 0 \quad (13)$$

Upon simplification, equation (13) becomes:

$$\frac{d^2\theta}{dX^2} - \frac{hPL^2}{kA_c}\theta = 0 \quad (14)$$

Let

$$m^2 = \frac{hPL^2}{kA_c} \quad (15)$$

Therefore,

$$\frac{d^2\theta}{dX^2} - m^2\theta = 0 \quad (16)$$

Let

$$\theta = e^{\gamma X}$$

Then

$$\frac{d\theta}{dX} = \gamma e^{\gamma X}$$

$$\frac{d^2\theta}{dX^2} = \gamma^2 e^{\gamma X}$$

Therefore, equation (16) becomes

$$\frac{d^2\theta}{dX^2} = m^2 e^{\gamma X} \quad (17)$$

$$\gamma^2 e^{\gamma X} - m^2 e^{\gamma X} = 0 \quad (18)$$

Upon simplification

$$\gamma = \pm m \quad (19)$$

The solution of the dimensionless temperature is then [22-23]:

$$\theta = Ae^{mX} + Be^{-mX} \quad (20)$$

Differentiating equation (20) yields;

$$\frac{d\theta}{dX} = mAe^{mX} - mBe^{-mX} \quad (21)$$

The heat dissipated from the thermoelectric modules is given as [24]:

$$Q_h = -\left(I^2R + \propto IT_h + k\frac{dT}{dx}\right) \quad (22)$$

Where I: current, A, R: resistance Ω, $\frac{dT}{dx}$: rate of temperature change with length, T_h: hot side temperature, ^oC.

Changing $\frac{dT}{dx}$ to a dimensionless parameter, defined as:

$$\frac{dT}{dx} = \frac{d\theta}{dX}\frac{(T_b - T_\infty)}{L} \quad (23)$$

Substituting equation (23) into equation (22) yields;

$$Q_h = -\left(I^2R + \propto IT_h + k\frac{d\theta}{dX}\frac{(T_b - T_\infty)}{L}\right) \quad (24)$$

Upon rearrangement

$$\frac{d\theta}{dX} = -\frac{(I^2R + \propto IT_h + Q_h)L}{(T_b - T_\infty)k} \quad (25)$$

For the design model, the fin tip temperature is conditioned to be equal to the ambient temperature. Applying first boundary condition when X=1, $\theta = 0$, equation (20) then yield;

$$Ae^m + Be^{-m} = 0 \quad (26)$$

$$A = -Be^{-2m} \quad (27)$$

Applying the second boundary condition,

when X= 0, $\frac{d\theta}{dX} = -\frac{(I^2R + \propto IT_h + Q_h)L}{(T_b - T_\infty)k}$, equation (21) then yield;

$$-\frac{(I^2R + \propto IT_h + Q_h)L}{(T_b - T_\infty)k} = -mBe^{-2m}e^{mX} - mBe^{-mX} \quad (28)$$

Collecting like terms,

$$-\frac{(I^2R + \propto IT_h + Q_h)L}{(T_b - T_\infty)k} = -mBe^{-2m+mX} - mBe^{-mX} \quad (29)$$

Further simplification yield

$$\frac{(I^2R + \propto IT_h + Q_h)L}{(T_b - T_\infty)k} = mB(e^{-2m+m(0)} + e^{-m(0)}) \quad (30)$$

Therefore, B becomes;

$$B = \frac{(I^2R + \propto IT_h + Q_h)L}{(e^{-2m})(T_b - T_\infty)km} \quad (31)$$

Substituting equation (31) in equation (27), yields

$$A = \frac{-(I^2R + \propto IT_h + Q_h)L(e^{-2m})}{(e^{-2m})(T_b - T_\infty)km} \quad (32)$$

Substitution of equation (31) and equation (32) into equation (20), the equation for the dimensionless temperature profile becomes;

$$\theta = \frac{-(I^2R + \propto IT_h + Q_h)Le^{-2m}.e^{mX}}{(e^{-2m})(T_b - T_\infty)km} + \frac{(I^2R + \propto IT_h + Q_h)Le^{-mX}}{(e^{-2m})(T_b - T_\infty)km} \quad (33)$$

Reducing the dimensionless temperature to its dimensional parameter, equation (33) becomes;

$$\frac{T - T_\infty}{T_b - T_\infty} = \frac{-(I^2R + \propto IT_h + Q_h)Le^{-2m}.e^{m\frac{x}{L}}}{(e^{-2m})(T_b - T_\infty)km} + \frac{(I^2R + \propto IT_h + Q_h)Le^{-m\frac{x}{L}}}{(e^{-2m})(T_b - T_\infty)km} \quad (34)$$

Upon Simplification and collection of like terms, equation (34), yields;

$$\frac{T - T_\infty}{T_b - T_\infty} = \frac{-(I^2R + \propto IT_h + Q_h)L}{(e^{-2m})(T_b - T_\infty)km}(e^{-2m+m\frac{x}{L}} - e^{-m\frac{x}{L}}) \quad (35)$$

Re-arrangement of equation (35) gives the temperature profile model of the plate fin heat sink as:

$$T = \frac{(I^2R + \propto IT_h + Q_h)L}{km(e^{-2m})}\left(e^{-m\frac{x}{L}} - e^{-2m+m\frac{x}{L}}\right) + T_\infty \quad (36)$$

With reference figure 3, the perimeter of the fin spacing can be expressed as [25]:

$$P = 2(H + s) \quad (37)$$

Where H is the height of the fin, m, s is fin spacing, m. If there are n number of fins the number of air gaps is (n-1), the width can therefore be expressed thus [6]:

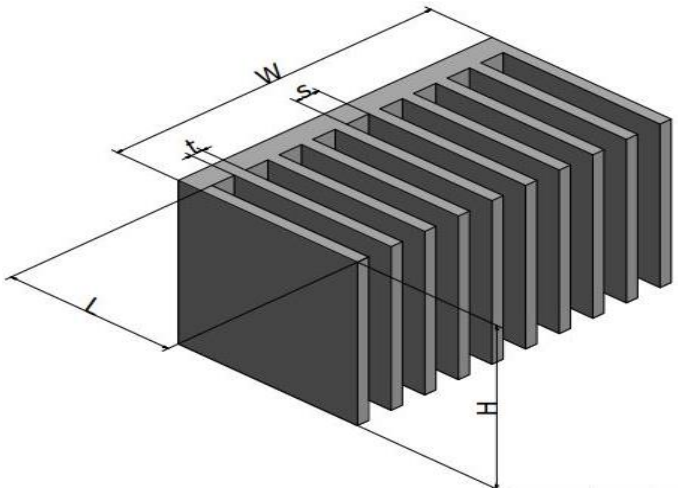

Figure 3: *Heat Sink Geometry*

$$w = nt + (n-1)s \tag{38}$$

The convective area is defined by the expression

$$A_c = 2 \times n \times l \times w \tag{39}$$

In the light of equation (37), equation (38) and equation (39), equation (15) becomes;

$$m = \sqrt{\frac{h(H+s)}{k[nl(nt+(n-1)s)]}} \tag{40}$$

To ensure efficient heat absorption and heat dissipation, the thermoelectric module is sandwiched between two heat sinks as shown in figure 4.

Figure 4: *Assemly of Heat Sink and Thermolectric Module*

The thermal absorption at the cold surface is expressed as [6]:

$$Q_c = \alpha I T_c - jI^2R \tag{41}$$

Where j is defined by the expression [25]:

$$j = \frac{1}{2} + \frac{k\,\Delta T}{I^2R} \tag{42}$$

$$Q_c = \alpha I T_c - \frac{I^2R}{2} - k\Delta T \tag{43}$$

Equation (36) is valid for the cold side heat sink, when X= 0, $\frac{d\theta}{dX} = -\frac{(I^2R+\propto IT_c+Q_c)L}{(T_b-T_\infty)k}$

Properties of air are evaluated at the mean film temperature defined by:

$$T_f = \frac{T_\infty + T_h}{2} \tag{44}$$

The Raleighs number is obtained from the relation [20]:

$$Ra = \frac{g\beta(T_h - T_\infty)w^3}{v^2}Pr \tag{45}$$

Pr is the Prandtl number, v is the kinematic viscosity, m^2/s,

$$\beta = \frac{1}{T_f}, /K$$

The Nusselts number Nu, is given by the expression [26]:

$$Nu = 1.911Ra^{0.31} \tag{46}$$

The convective heat transfer coefficient is readily obtained from [27-28]:

$$Nu = \frac{hl_e}{k} \tag{47}$$

where l_e is the characteristic length and equals to be the height of the heat sink. For n couples in a module; α, $(R)n$, and $(k)n$ can be approximated as [29]:

$$\alpha = \frac{V_{max}}{T_h} \tag{48}$$

$$(R)n = \frac{T_h - \Delta T_{max}}{T_h}\frac{V_{max}}{I_{max}} \tag{49}$$

$$(k)n = \frac{T_h - \Delta T_{max}}{2\Delta T_{max}}\frac{V_{max}I_{max}}{T_h} \tag{50}$$

Where V_{max} is the module maximum voltage, V, I_{max} is the module maximum current, A, ΔT_{max} is the maximum gradient difference K.

3.0 METHODOLOGY

A model of the heat sink was derived analytically and solved exactly using MATLAB to depict pictorial representation of its temperature profile at different fin spacing, fin thickness, fin length and number of fins while coupling the heat sink model to the heat absorbed and dissipated model of the TEC 1-12706 modules. The thermophysical properties of air employed for simulation are; dynamic viscosity 1.773 kg/ms, thermal conductivity 2.506 kW/mK, heat transfer coefficient 1.787 W/m2K, Prandtl number 0.7106, density 1.455 kg/m3, specific heat at constant pressure and at constant volume are 1.004 kJ/kgK and 0.7167 kJ/kgK respectively. The length and width of the heat sink is chosen to completely enclosed ten TEC 1-12706, 12Vand 60W thermoelectric modules with the dimensions 40mm x 40mm x 4mm. The model was optimized using the FMINCON, optimization in MATLAB.

The refrigerated model space is a cube of 400mm in dimension maintained at -2°C. Figure 5 shows an assembly of the thermoelectric modules, hot and cold side heat sinks.

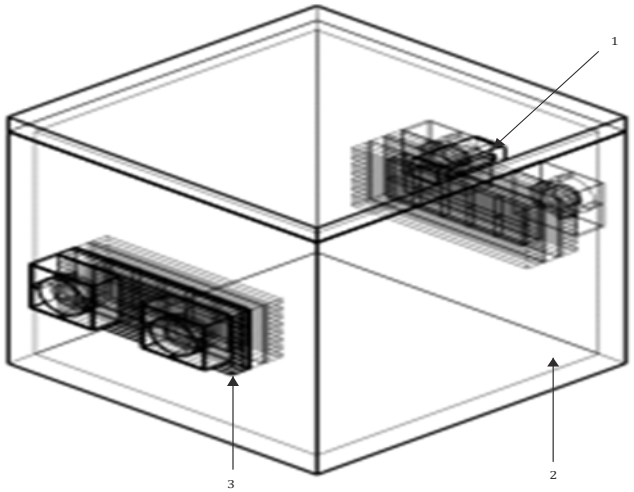

Figure 5: *Assembly of Modules, Heat sink and Refrigerated Chamber*

1: Right hand heat sink module assembly with cooling fans 2: Refrigeration Chamber 3: Left hand heat sink assembly with cooling fans

4.0 RESULTS AND DISCUSSION

4.1 Temperatures of Hot and Cold Side Heat Sink versus Number of Fins at different Fin Lengths

Figure 6 shows the graphical representation of the temperature profile of the hot and cold side heat sink with fin numbers and fin lengths at constant fin spacing of 5mm and fin thickness of 4mm. Increasing the fin numbers lead to a reduction in temperature while increasing the fin lengths lead to an increase in temperature.

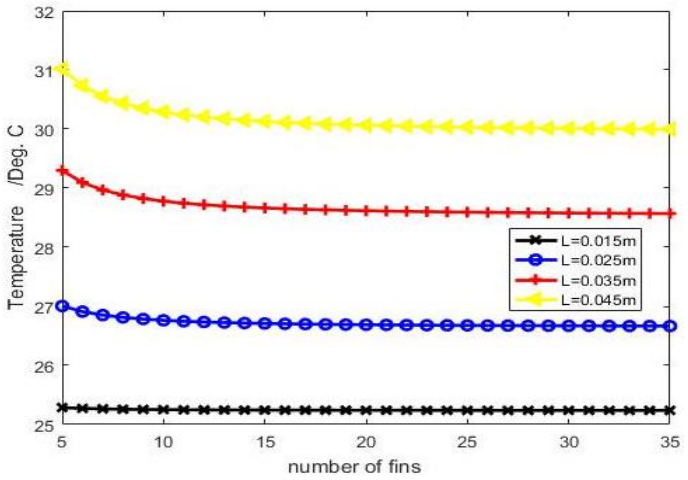

(a)

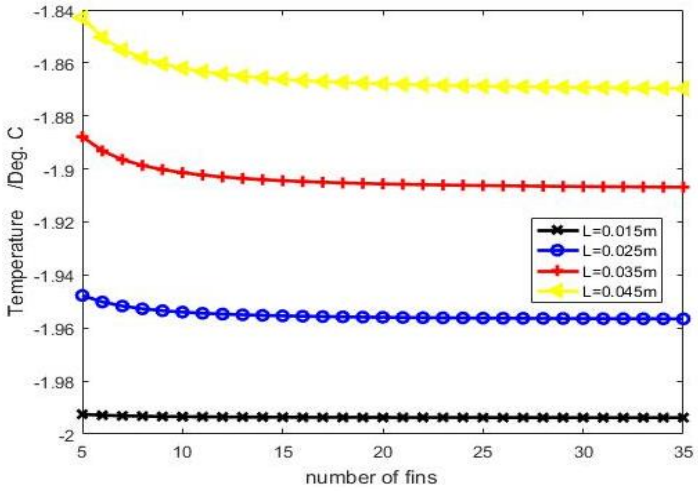

(b)

Figure 6: *Temperature Profile of Heat Sink (a) Hot Side (b) Cold Side vs Number of Fins at various Fin Lengths*

The increase in fin numbers increase the total convective surface area, hence a reduction in the fin temperature. Increase in fin length lead to a greater pressure drop which tends to reduce the air flow in the fin spacing causing an in increase in fin temperature. It can be infer that increase in number of fins and fin lengths positively imparted the thermal dissipation ability of the heat sink. However, at constant number of fins, increases in fin length lead to increases in surface temperature of the heat sink.

4.2 Temperatures of Hot and Cold Side Heat Sink versus Number of Fins at different Fin Spacing

Figure 7 shows the graphical representation of the

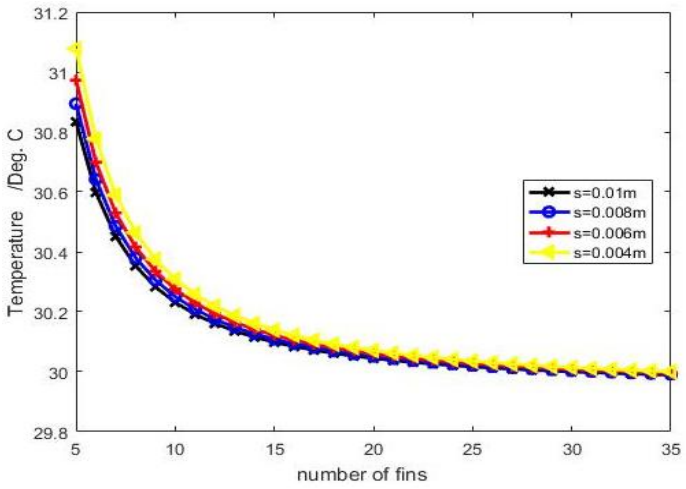

(a)

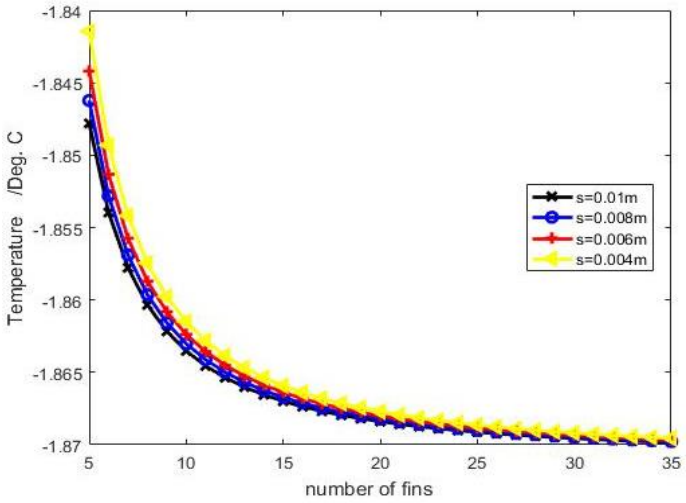

(b)

Figure 7: *Temperature Profile of Heat Sink (a) Hot Side (b) Cold Side vs Fin Numbers at various Fin Spacing*

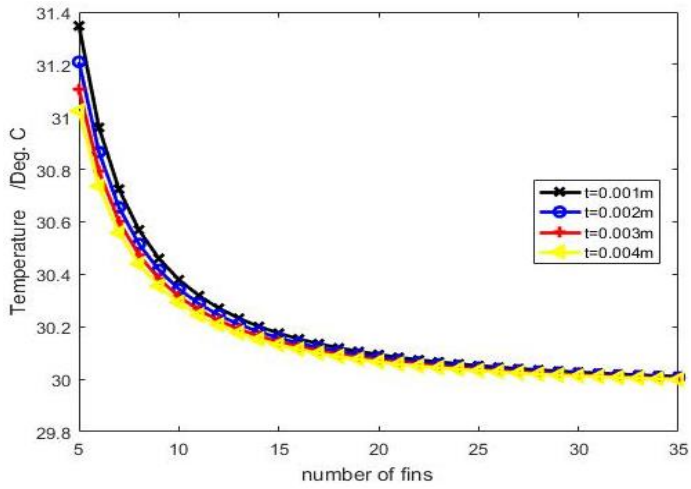

(a)

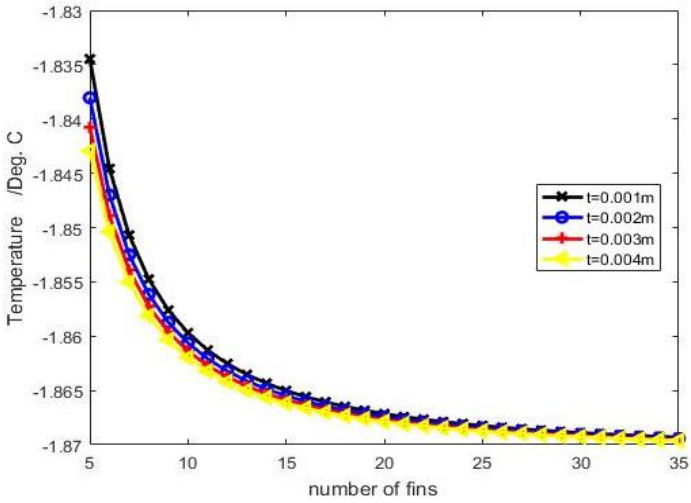

(b)

Figure 8: *Temperature Profile of Heat Sink (a) Hot Side (b) Cold Side vs Number of Fins at various Fin Thickness*

effect of fins and fin spacing on temperature profile of hot and cold heat sink at constant fin length of 45mm and thickness of 4mm. The temperature is seen to decrease with increase in number of fins and an increase in fin spacing.

The effect of fin spacing is however not very significant and becomes almost negligible as the fin spacing is increased. Increases in fin spacing result in decreases of the thickness of the boundary layer which improves the heat transfer coefficient and thus an effective heat dissipation.

4.3 Temperatures of Hot and Cold Side Heat Sink versus Number of Fins at different Fin Thickness

Figure 8 shows the graphical representation of the effect of number of fins and fin thickness on the temperature profile of hot and cold sides heat sink at constant fin length of 45mm and fin spacing of 5mm. The temperature decreases exponentially while increasing the fin numbers and increasing the fin thickness.

In the analysis, clearly there is interdependency between the number of fins, fin spacing, fin thickness and fin length on performance of the heat sink. Increases in the number of fins have the effect of either decreasing the spacing or thickness of the fins while increases in the fin length will lead to more fan power and greater pressure gradients which will in turn affect the overall heat transfer coefficient. Increases in fin spacing and thickness improves heat transfer coefficient while decreases in fin length and number of fins improves heat transfer coefficient which will positively impart the performance of the thermoelectric cooler modules. As a result, the heat sink need be optimized using the genetic algorithm based on biologic evolution. the optimization was done using FMINCON tool in OPTIMTOOL box in MATLAB. The temperature profile of

equation (36) is the objective function, the heat sink parameters; number of fins, fin spacing, fin thickness and fin length are the constraints which are bounded by upper and lower values to satisfy space and volume requirement of the refrigerated chamber. Table 1 list the optimised heat sink parameters of the number of fins, fin spacing, fin thickness, and fin length, with an optimum temperature of -0.8639.

Table 1: Optimized Fin numbers, Fin thickness, Fin spacing and Fin length

n	t /m	s /m	L /m
10	0.002	0.003	0.015

5.0 CONCLUSION

Thermoelectric refrigeration is a type of refrigerator that achieves cooling through Peltier and Seebeck effect. Heat sinks efficiently transfers the heat absorbed from the cold junction to the surrounding using air. The heat sink was thus mathematically modelled and optimized to ensure optimal performance of a thermoelectric refrigerator. The derived model was solved and optimized using FMINCON optimisation tool in MATLAB, to depict the behaviour of the heat sinks at cold side and ambient temperature of -2^{o}C and 28^{o}C respectively. The optimum values for the hot and cold heat sink geometry obtained using FMINCON tool in OPTIMTOOL box in MATLAB, yields number of fins as 10, fin spacing as 0.003m, the fin thickness as 0.002m and fin length as 0.015m with an optimum temperature of -0.8639.

REFERENCES

[1] Patond S. B., Bhadake P. G., Patond C. B. "Experimental Analysis of Solar Operated Thermo-Electric Heating and Cooling System", *International Journal of Engineering Trends and Technology*, 20(3), 2015, pp. 125-150.

[2] Totala N. B., Desai V. P., Rahul K. N. S., Debarshi G., Mohd S. Y., Jane N. S. "Study and Fabrication of Thermoelectric Air cooling and Heating System, *International Journal of Engineering Inventions*, 4(2), 2014, pp 20-30.

[3] Mani, P. I. "Design, Modelling and Simulation of a Thermoelectric Cooling System", Master Thesis, Western Michigan University. United States of America .

[4] Duragkar S. , Khodaskar R. , Junankar A. , Khadgi J. , Dhumal V.M., "Implementation of Solar Fridge and Fast Chilling using Peltier Effect with Temperature Monitoring", *International Journal of Engineering , Science and computing*, 7(4), 2017, pp. 6235-6237.

[5] Badgujar G. S., Patil A. A., Patil V. H. "To Enhance Heat Transfer Rate in Cooler", *International Journal of Innovations in Engineering and Technology*, 5(4), 2015, pp 42-46.

[6] Karathanassis I.K, Papanicolaou E., Belessiotis V., Bergeles G., "Multi-objective Design Optimization of a Micro Heat Sink for Concentrating Photovoltaic/Thermal (CPVT) System Using a Genetic Algorithm" *Applied Thermal Engineering*, 59(1), 2015, pp. 733-744.

[7] Raju A., Ajeesh J., Akash S., Akhil T. J., Bose V., Jinshah B. S. "Development of a Portable Solar Thermoelectric Refrigerator", *International Journal of Scientific and Engineering Research*, 7(4), 2016, pp. 426-428.

[8] Lee M., Kim H. J., Kim K. "Nusselt Number Correlation for Natural Convection from Vertical Cylinder with Triangular Fins", *Applied Thermal Engineering*, 93, 2016, pp. 1238-1247.

[9] Micheli L., Reddy K., Mallick T. K. "Experimental Comparison of Micro-scaled Plate-fins and Pin-fins under Natural Convection International Community", *Heat and Mass Transfer*, 75, 2016, pp. 59-66.

[10] Yu X., Feng J., Feng Q., Wang Q. "Development of a Plate-pin fin Heat Sink and its Performance Comparisons with a Plate-fin Heat Sink", *Applied Thermal Engineering*, 25(2), 2005, pp. 173-182.

[11] Wang C., Hung C., Chen W. "Design of heat sink for Improving the Performance of Thermoelectric Generato using two stage Optimization", *Energies*, 39, 2012, pp. 236-245.

[12] Szodrai F. "Heat Sink Shape and Topology Optimization with Pareto-Vector Length Optimization for Air Cooling", *Energies*, 13(1661), 2020, pp. 1-15.

[13] Lin C., Kiflemariam R. "Numerical Simulation and Validation of Thermoelectric Generator Based Self-Cooling System with Airflow", *Energies*, 12,4052, 2019, pp. 1-21.

[14] Bokde P. G., Jibhakate Y. M. "Design Construction and Performance evaluation of Solar operated Dual Purpose Refrigerator using thermoelectric module", *International Journal for Research in Applied Science and Engineering Technology*. 4(7), 2016, pp 320- 326.

[15] Da Rosa A. V. "Fundamentals of Renewable Energy Processes", *Elsevier Academic Press*, USA, 2005, pp. 149-150.

[16] Chaudhary U. K., Patel A., Arya D., Gautam D., Choudhary P. "Solar Refrigeration using Peltier Module", *International Journal of Engineering and techniques*, 4(2), 2018, pp 804 808.

[17] Dhawade M. B., Mourya E., Yadav A., Samuel D., Mohod S. A., Deshpande V. N. Review on Portable Solar Thermoelectric Refrigerator Cum Air Cooler, *International Journal of Advance Research in Science and Technology*, 4(10), 2015, pp 44-58.

[18] Awasthi M., Mali K. V. "Design and Development of Thermoelectric Refrigerator", *International Journal of Mechanical Engineering and Robotics Research*, 2012, pp 389-399.

[19] Lee S. "Optimum Design and Selection of Heat Sinks", *11th Institute of Electrical and Electronics Engineers Transaction on Components Packaging and Manufacturing Technology, 18(4),* 1995, *pp. 812-817.*

[20] Cengel Y.A. "Heat Transfer: A Practical Approach", 2nd edition *McGraw Hill Higher Education*, 1997, pp. 470-480.

[21] Rajput R. K. "Heat and Mass Transfer" S. Chand and Company Ltd. Ram Nagar, New Delhi- 110065, 1999, pp. 506 – 538.

[22] Stroud K. A., Booth D. J. Engineering Mathematics. 5th Edition, Palgrave, Great Britain, 2001, pp. 1073-1074.

[23] Kreyszig E. *Advanced Engineering Mathematics*. 8th Edition, John Wiley and Sons Inc. New York, 2003, pp. 72-75.

[24] Mehmedagic I., Krug J. "Heat Sink Design and Optimization". *U.S Army Armament Research, Development and Engineering Center*, AD-E403716, pp 1 – 24.

[25] Clifton W. E. "Thermoelectric Cooler Design", Master Degree Thesis, Department of Astronautical Engineering, Naval Postgraduate School, USA, 1992

[26] Walung A. A., Daund V. S., Palande D. D. "Review of Performance of Rectangular Fins under Natural Convection at Different Orientation of Heat Sink", *International Journal of Innovation and Applied Studies*, 6(2), 2014, Pp. 232-238.

[27] Eastop T. D., McConkey A. *Applied Thermodynamics: Engineering Technologists*. 5th Edition, Pearson Education, 2004, pp. 599-602.

[28] Rogers G., Mayhew Y. *Engineering Thermodynamics: Work and Heat Transfer*. 4th Edition, Pearson Education, 2003, pp. 555-557.

[29] Rawat M. K., Sen P. K., Chattopadhyay H., Neogi S. "Development and Experimental Study of Solar Powered Thermoelectric Refrigeration System", *International Journal of Engineering Research and Applications*, 2013, pp. 2543-2547.